Differences in the Volume Distributions of Human Lung Mast Cell Granules and Lipid Bodies: Evidence That the Size of These Organelles is Regulated by Distinct Mechanisms

ILAN HAMMEL,*‡ ANN M. DVORAK,* STEPHEN P. PETERS,§ EDWARD S. SCHULMAN,§ HAROLD F. DVORAK,* LAWRENCE M. LICHTENSTEIN,§ and STEPHEN J. GALLI*

*From the *Departments of Pathology, Beth Israel Hospital and Harvard Medical School, and the Charles A. Dana Research Institute, Beth Israel Hospital, Boston, Massachusetts 02215; ‡the Department of Pathology, The Sackler School of Medicine, Tel Aviv University, Ramat Aviv, Tel Aviv, Israel; and §the Department of Medicine, Division of Clinical Immunology, the Johns Hopkins University School of Medicine at the Good Samaritan Hospital, Baltimore, Maryland 21239. Address correspondence to S. J. Galli.*

ABSTRACT We analyzed transmission electron micrographs of human lung mast cells by digitized planimetry and point counting to determine the cross-sectional areas of two distinct cytoplasmic organelles: specific granules and lipid bodies. Specific granules have a limiting membrane and often contain one or more cylindrical scroll-like inclusions. By contrast, lipid bodies are on average much larger than granules and lack both limiting membranes and inclusions. The measured cross-sectional areas of lipid bodies and scroll-containing granules were converted to equivalent volumes, and the noise in the frequency distribution of these volumes was smoothed using a moving bin technique. This analysis revealed (*a*) a periodic, multimodal distribution of granule equivalent volumes in which the modes fell at volumes that were integral multiples of the volume defined by the first mode (the "unit volume"), and (*b*) a modal granule equivalent volume frequency that occurred at a magnitude equal to four "unit volumes." Thus, specific granules appear to be composed of units of a narrowly fixed volume. Furthermore, the mean volume of intragranule inclusions was 0.0061 μ^3, a value very similar to that calculated for the "unit volume" (0.0071 μ^3). This result suggests that each "unit volume" comprising the individual scroll-type granules contains (or is capable of generating or accommodating) a single scroll-like inclusion. In contrast to the specific granules, mast cell lipid bodies lack a periodic, multimodal volume distribution. Taken together, these findings suggest that the volumes of human lung mast cell granules and lipid bodies are regulated by distinct mechanisms.

The volume of rat mast cell cytoplasmic granules exhibits a periodic, multimodal distribution in which the modes represent successively larger integral multiples of the volume at the first mode (14). One model to account for this finding is that rat mast cell granules are composed of an integral number of units ("unit granules") whose volume is defined by the first mode in the granule volume distribution.

If correct, this model defines a previously unappreciated aspect of mast cell secretory granule structure, with potentially important implications for the understanding of mechanisms regulating the size of these organelles. We now have tested this model by analyzing human lung mast cells. Human mast cells are particularly suitable for morphometric studies of granule organization. Unlike rat mast cell granules, whose content appears homogeneously electron dense, human mast cell granules often have discernible substructural elements, such as scroll-like inclusions (2, 8, 12, 16). We reasoned that quantitative analysis of these inclusions might reveal aspects of mast cell granule organization that were inaccessible in the rat. Also, human mast cells differ from rat mast cells in containing numerous cytoplasmic lipid bodies (or "lipid droplets", as cited in references 7, 8, and 12). Lipid bodies generally

THE JOURNAL OF CELL BIOLOGY · VOLUME 100 MAY 1985 1488-1492

are much larger than specific granules and may be distinguished from granules by their lack of a limiting membrane and by their homogeneously electron-dense content. By analogy to the lipid bodies of adipocytes (10), we expected that the size of mast cell lipid bodies might depend upon the gradual accumulation and/or loss of cellular lipid, a natural history unlikely to give these structures a periodic, multimodal volume distribution. We therefore examined lipid bodies as a potential "control" organelle whose analysis might provide a counterpoint to our quantitative studies of the specific cytoplasmic granules.

In this report, we present evidence supporting the notion that human mast cell granules are composed of integral units, and show that this model does not account for the volume distribution of mast cell cytoplasmic lipid bodies.

MATERIALS AND METHODS

Mast Cells: To isolate human lung mast cells, we dispersed single cells from lung fragments by incubation with the proteases Pronase, chymopapain, collagenase, and elastase as previously described (8, 22). These preparations (2–10% mast cells) were purified further by countercurrent centrifugation elutriation (22), in some cases followed by centrifugation over discontinuous Percoll gradients. A "100% Percoll" solution was prepared by mixing 9 parts Percoll and 1 part (vol/vol) 10× Hanks' balanced salt solution (GIBCO Laboratories, Grand Island, NY). This Hanks' balanced salt solution (GIBCO Laboratories) was then used to prepare 40, 50, 60, 70, and 80% Percoll solutions by dilution with 1× Hanks' solution. Then we suspended 10–20 million cells in 1 ml of "100% Percoll" and pipetted them into the bottom of a 12 × 100-mm Falcon test tube; on top of this we carefully layered 0.8 ml each of 80, 70, 60, 50, and finally 40% Percoll. These preparations were then centrifuged at 1,400 rpm (400 *g*) at 27°C for 10 min. Cells at each interface were collected separately for determination of cell number and viability. Mast cells were washed with a buffer composed of 25 mM piperazine-*N*,*N*′-bis-2-ethanesulfonic acid (Sigma Chemical Co., St. Louis, MO), 140 mM NaCl, 6 mM KCl, 0.003% human serum albumin (Miles Laboratories Inc., Elkhart, IN), and 0.1% glucose. The experiments reported here were performed with preparations containing 20–74% mast cells.

Transmission Electron Microscopy: Cells isolated from three different patients were fixed in suspension (8, 9), postfixed in collidine-buffered osmium tetroxide, stained en bloc in uranyl acetate, dehydrated in a graded series of alcohols, and embedded in Epon (6) as previously described (8). Specimens were examined in a Phillips 400 electron microscope (8). Photomicrographs of 65 mast cells printed at a final magnification of 20,000× were used for quantitative analysis.

Quantitative Analysis of Mast Cell Granules and Lipid Bodies: The rationale of our analytical approach has been described in detail (14). Briefly, we wished to test the hypothesis that mast cell granules are composed of variable numbers of discrete units. If this model is correct, and if the individual discrete units have a narrowly fixed volume (which we refer to operationally as the "unit volume"), then the volumes of individual granules would vary as integral multiples of the "unit volume." The most straightforward way to test this model would be to measure the volume of individual mast cell granules directly. As this approach was not possible, we instead characterized the volumes of mast cell granules using direct measurements of their cross-sectional areas as revealed in electron micrographs. For structures whose shape approximates that of a sphere (as does the shape of human lung mast cell granules), measurements of organelle cross-sectional areas may be converted to their "equivalent sphere volumes," and the results used to generate a histogram showing the frequency distribution of the "equivalent volumes" (14, 15, 27). A standard data smoothing method which has enjoyed widespread use in the physical and biological sciences (the "moving bin" technique, as in references 14, 18, 19, 23, and 24) is then applied to reveal true peaks in the equivalent volume frequency distribution. It is important to emphasize that while this approach can accurately determine that a particular population of spherical structures contains multiple subpopulations whose volumes vary by integral amounts, neither it nor any other currently available method (1, 23, 26) can reveal the precise relative frequency of each of the subpopulations.

Selection of mast cells for preparation of photomicrographs was based on quality of preservation of cell structure. Most images of mast cells (e.g., Fig. 1)

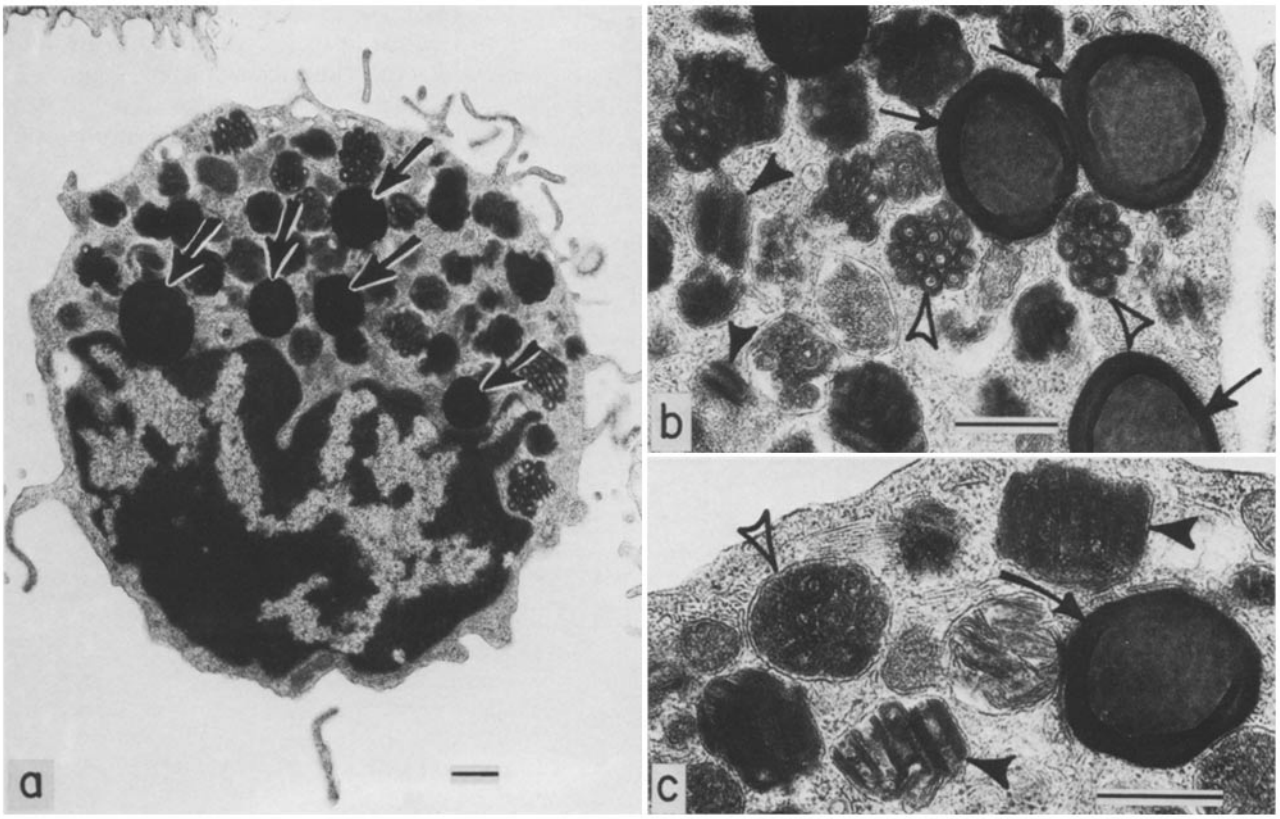

FIGURE 1 (*a*) Mast cell purified from human lung. Note the many cytoplasmic granules and the larger, homogeneously electron-dense lipid bodies (arrows). (*b* and *c*) Higher power electron micrographs illustrate cytoplasmic lipid bodies (arrows) and granules with scroll-like inclusions cut in cross section (empty arrowheads) or longitudinally (filled arrowheads). Bars, 0.5 μm. (*a*) × 12,600; (*b*) × 27,000; (*c*) × 35,000.

included part of the nucleus and one or more cytoplasmic lipid bodies; all included multiple specific cytoplasmic granules. Human mast cell granules may exhibit a variety of substructural patterns (2, 8, 12, 16). An individual mast cell may contain some granules with one substructural pattern and some with others, but in most cases granules of one particular pattern predominate. In our material, most mast cells had granule populations primarily of the "scroll" substructure (Fig. 1). For the work reported here, we restricted the quantitative analysis to mast cells with a predominantly scroll-type granule substructure (~90% of the mast cells present). In each mast cell photographed, every unequivocally identifiable cytoplasmic granule and cytoplasmic lipid body was analyzed.

As an expression of organelle shape, we determined the distribution of granule or lipid body axial ratios and compared them with the distributions expected for ideal prolate or oblate spheroids (spheroids extended or flattened at the poles, respectively) with an axial ratio of 2. Organelle axial ratios were determined by using a MOP-3 digitizer (Carl Zeiss, Inc., Thornwood, NY) interfaced to an HP86 computer (Hewlett-Packard Co., Palo Alto, CA) to record organelle perimeter, profile area (A), and largest diameter (major axis = a). The length of the minor axis (b) was calculated according to the formula $b = 4A/\pi a$. Both granules and lipid bodies had mean axial ratios (b/a) of ≤1.3 (see below) and as a result were treated as spheres for purposes of volume calculations (15, 27).

To estimate granule, lipid body, nucleus, and cell volumes, we first determined their profile areas (A) by digitized planimetry as described above, then calculated the mean diameters of individual profiles (d) from the areas ($d = 2\sqrt{A/\pi}$). The mean of these profile diameters ($\bar{d}$) was then calculated and used to calculate the mean organelle diameter ($\bar{D} = 4\bar{d}/\pi$) (see references 20 and 27). This value was confirmed by the Fullman method (11), in which $\bar{D}$ is estimated from the harmonic mean profile diameter ($\bar{D} = N\,\pi/2\,(1/d_1 + 1/d_2 + \cdots + 1/d_N)$, where N = number of profiles). The mean organelle or cell volume ($\bar{v}$) was then calculated from the mean profile area ($\bar{A}$) using the Weibel and Gomez (25) formula: $\bar{v} = 1.4(\bar{A})^{3/2}$, and confirmed by $\bar{v} = \pi\bar{D}^3/6$.

Volume fraction (V_v) of organelles was estimated from their areas as determined by point counting using a screen of 1 point/cm^2 (27). The numerical organelle density (N_v) was determining using the mean of values generated by two methods: that of DeHoff and Rhines (5) ($N_v = N_a/\bar{D}$) and that of Loud et al. (17) ($N_v = V_v/\bar{v}$). Organelle area density (N_a) was calculated by dividing the number of all observed granules by the total cytoplasmic area.

To determine whether granule or lipid body volumes were distributed in a multimodal fashion, we analyzed their sizes by the "moving bin" method (14, 18, 19, 21, 24). For this analysis, the measured organelle profile areas were first transformed into equivalent sphere units ($v = 4\pi[d/2]^3/3$). A primary histogram was then constructed showing the number of organelles recorded at various equivalent volumes. The noise in this frequency distribution was then smoothed by plotting histograms showing the linear sums of the frequencies recorded for all volumes occurring between values differing by a fixed amount (the "bin size"), calculated as the bin was moved sequentially in small fixed increments (the "bin increment") over the entire range of recorded equivalent volumes. We analyzed the primary histogram of organelle equivalent volumes using at least six different combinations of bin sizes and bin increments, and recorded the data as histograms using a HP 7470 plotter (Hewlett-Packard Co.). In this method, peaks in the frequency distribution are considered real if they appear at approximately the same location irrespective of bin size (14, 18, 19, 21). If a multimodal distribution is revealed, its periodicity (which defines the size of the "unit volume") is extrapolated as the mean of the intermodal spaces.

To estimate the volume of the scroll-like granule inclusions, we assumed that their shape approximated that of an ideal cylinder. This assumption is consistent both with the results of previous ultrastructural analyses of these inclusions (2, 8, 12, 16) as well as with inspection of our own photomicrographs (Fig. 1). We determined the cross-sectional area (A_s) of all scrolls that presented nearly circular profiles, i.e., were sectioned perpendicular to their long axis (Fig. 1 *b*), and the length (l) of all scrolls sectioned along their long axis (Fig. 1 *b*). Scroll cross-sectional areas and lengths were plotted as histograms, and the mean scroll volume (v_s) was calculated according to the formula $v_s = \bar{A}_s\bar{l}$.

TABLE I

*Quantitative Comparisons of Human Lung Mast Cell Cytoplasmic Granules and Lipid Bodies**

Characteristic	Granules	Lipid bodies
Axial ratio	1.32 ± 0.10	1.21 ± 0.14
Volume ($\bar{v}$) (μ^3)	0.025 ± 0.008	0.38 ± 0.18
N_v (U/μ^3 of cytoplasm)	4.39 ± 0.21	0.23 ± 0.02
U/cell	1352 ± 81	71 ± 5

* Determination of axial ratios, $\bar{v}$, and N_v based on an analysis of 24 mast cells (for granules) or 65 mast cells (for lipid bodies). The cellular volume (391 ± 20 μ^3) and nuclear volume (83 ± 5 μ^3) were calculated by analyzing 150 mast cell profiles (see Materials and Methods). Data are shown as mean ± SEM.

RESULTS

Analysis of the axial ratios of cytoplasmic granules (mean axial ratio ~ 1.3) and lipid bodies (mean axial ratio ~ 1.2) confirmed that these organelles are similar in shape, with configurations more closely approximating those of ideal prolates than ideal oblates. Mast cells contained 20-fold more granules than lipid bodies, but lipid bodies greatly exceeded granules in mean size (Table I).

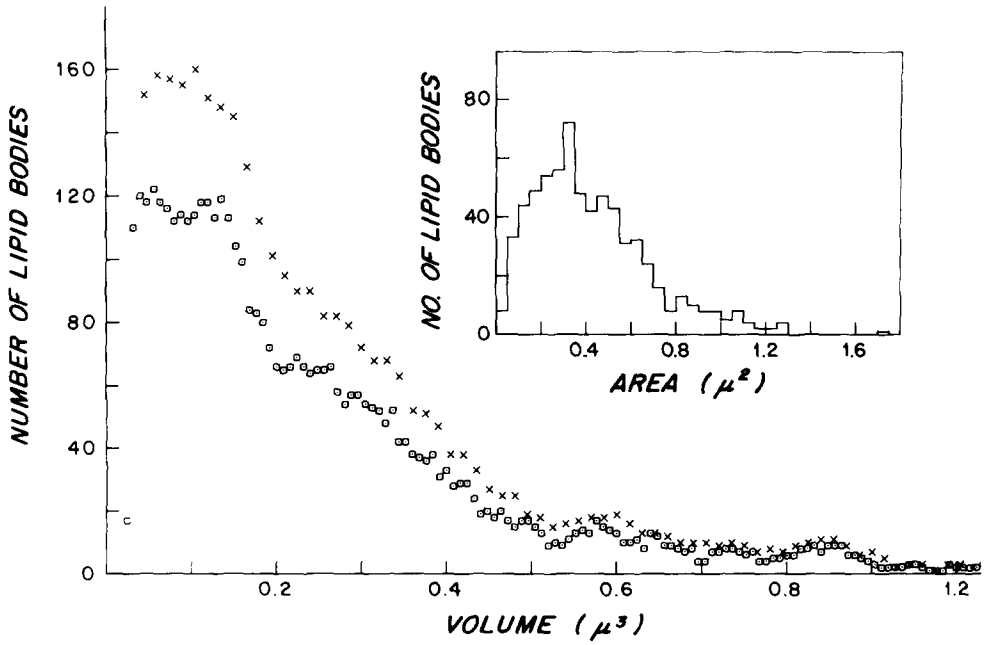

FIGURE 2 Moving bin histograms of lipid body equivalent volumes calculated with two different bin sizes (× = bin size 0.075 μ^3 moved every 0.015 μ^3; ⊡ = bin size 0.056 μ^3, moved every 0.008 μ^3). The distribution lacks true peaks. The inset shows the area distribution of measured lipid body cross-sectional areas. 672 lipid bodies (in 65 mast cells) were analyzed.

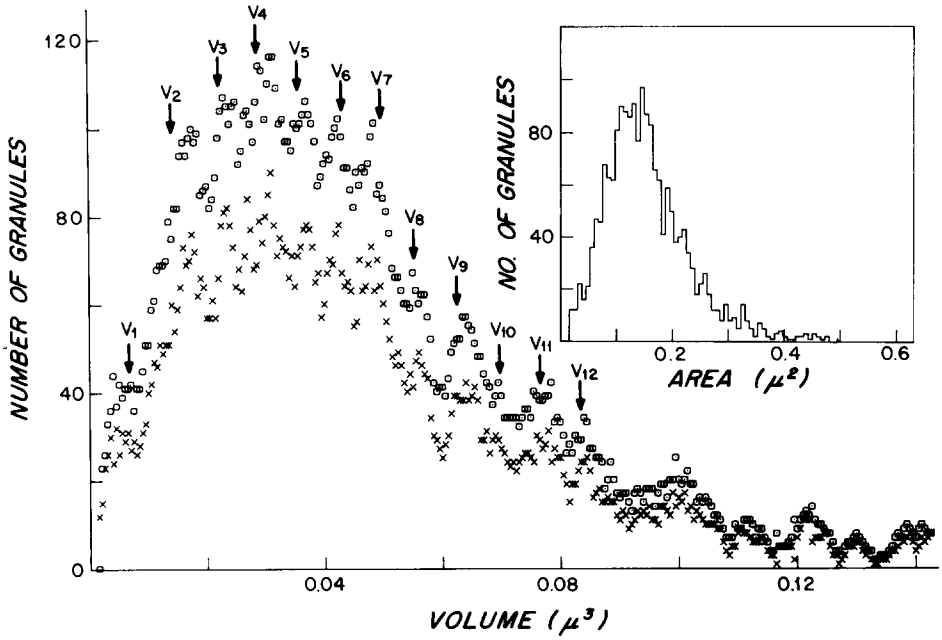

FIGURE 3 Moving bin histograms of cytoplasmic granule equivalent volumes. The distribution contains true peaks, which appear in the same positions in the histograms generated using two different bin sizes (× = bin size 0.0035 μ^3, moved every 0.0005 μ3; ⊡ = bin size 0.0025 μ^3, moved every 0.0005 μ^3). The arrows (v_1, v_2, v_3, etc.) are placed at integral multiples of the mean intermodal distance, a value that defines the magnitude of the "unit volume." The inset shows the distribution of measured granule cross-sectioned areas. 1882 granules (in 19 mast cells) were analyzed.

TABLE II

Estimates of Unit Volume (v_1) of Human Lung Mast Cell Volumes*

Mode	Bin size (μ^3):	0.0020	0.0028	0.0025	0.0035	0.0024	0.0042
(no.)	Bin increment (μ^3):	0.0004	0.0004	0.0005	0.0005	0.0006	0.0006
1		0.0060	0.0068	0.0065	0.0070	0.0060	0.0066
2		0.0064	0.0070	0.0080	0.0080	0.0081	0.0084
3		0.0077	0.0077	0.0078	0.0074	0.0059	0.0059
4		0.0068	0.0067	0.0068	0.0068	0.0079	0.0080
5		0.0074	0.0044	0.0074	0.0068	0.0073	0.0073
M		0.0069	0.0071	0.0073	0.0074	0.0070	0.0072
± SEM		0.0003	0.0002	0.0003	0.0002	0.0005	0.0005

* The unit volume (v_1) was calculated by determining the volume defined by the mode of each successive peak (V_1–V_5) in the granule equivalent volume distributions, as revealed by analysis with the indicated bin sizes and bin increments. The volume identified by the mode of each peak then was divided by the number of that peak to calculate v_1 for each peak ($v_1 = V_x/x$). The mean ± SEM of v_1 (the grand v_1) calculated from the mean values obtained using the six different combinations of bin size and bin increment = 0.0071 ± 0.0001 μ^3.

The area distribution of lipid body profiles, and two typical moving bin analyses of the corresponding lipid body equivalent volume distribution, are shown in Fig. 2. Moving bin analyses using six different bin sizes and three different bin increments did not reveal a multimodal distribution of lipid body equivalent volumes. By contrast, analysis of cytoplasmic granules clearly demonstrated a periodic, multimodal volume distribution. Fig. 3 graphically presents the results of moving bin analyses of granule equivalent volume distribution using two different combinations of bin size and bin increment. The same results were obtained with all 10 combinations of bin size and bin increment tested; the data from six of these analyses, including the two shown in Fig. 3, are summarized in Table II. Note that the peaks in the granule equivalent volume distribution occurred at nearly identical intervals for all the separate analyses (v_1 = 0.0069–0.0074 μ^3; grand v_1 = 0.0071 ± 0.0001 μ^3), confirming that the peaks in the volume distribution were real. The validity of the peaks was also confirmed by the observation that they occurred in the same location when the entire granule population (prints derived from all three patients) or subpopulations (prints from each of the three patients taken individually) were analyzed separately (data not shown). As shown in Fig. 3, the modal frequency of the granule equivalent volumes occurred at v_4 (0.028 μ^3).

The dimensions of individual intragranule scrolls are shown in Fig. 4. The mean volume of these structures was 0.0061 μ^3.

DISCUSSION

The volume distribution of human lung mast cell cytoplasmic granules exhibits multiple modes. A similar finding was obtained with rat peritoneal mast cell granules (14). In both studies, the results satisfied criteria identifying periodic volume distributions that reflect real characteristics of the granule populations and not merely random variation due to insufficient sampling of a population of organelles exhibiting a continuous and smooth size distribution (14, 18, 19). Thus, the modes of successive peaks fell at magnitudes representing integral multiples of the mode for the smallest peak, the

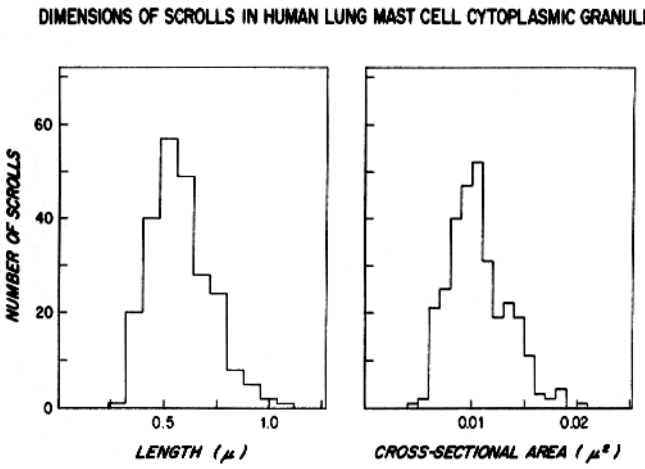

FIGURE 4 Histograms showing the lengths of all intragranule scrolls cut in longitudinal section, and the cross-sectional areas of all scrolls cut in perpendicular. Ten mast cells were analyzed.

spacing between adjacent peaks was constant and was equivalent to the volume defined by the mode of the smallest peak, and the positions of the peaks remained constant when the data were analyzed using multiple (in our case, 10) different combinations of bin sizes and bin increments. In addition, the positions of the peaks were independent of the size of the granule population measured.

Several models of granule formation and/or enlargement could account for a periodic, multimodal granule volume distribution. One hypothesis would be that the Golgi region produces granules of different sizes whose volumes vary as the integral multiple of the smallest volume. Another hypothesis, which we find rather more attractive, is that granules progressively enlarge by the addition of units whose volume corresponds to that of the smallest mode (the "unit volume"). Put differently, this model postulates that mast cell granule growth continues even after the formation of the primary or "unit" granule (by progranule fusion) (3, 4, 13) in the Golgi region.

In rat peritoneal mast cells, the only evidence compatible with granule-granule fusion that was evident from inspection of the electron photomicrographs was the occurrence of occasional pear- or dumbbell-shaped granules (14). In human lung mast cells, however, even granules with roughly circular profiles often contained one or more discrete substructural "units": cylindrical, scroll-like inclusions (2, 8, 12, 16). On a hunch that the volume of these inclusions might bear some relationship to that of the "unit volume," we directly measured all scrolls cut in favorable planes of section. Although the scrolls exhibited considerable individual variation, particularly in length (Fig. 4), their mean volume (0.0061 μ^3) closely corresponded to that calculated for the "unit volume" (0.0071 μ^3). The precise relationship between the scroll-like inclusion and the "unit granule" remains to be determined. One possibility is that the putative "unit granule" contains material sufficient, under appropriate circumstances, to generate a single scroll. However, the scroll does not represent an obligatory and/or unchangeable feature of the human lung mast cell "unit granule," because most mast cells have at least some granules which appear devoid of these structures (2, 8, 12, 16).

In addition to specific cytoplasmic granules, human lung mast cells also contain cytoplasmic lipid bodies. Although these two organelles are similar in shape, lipid bodies are distinguishable from cytoplasmic granules by their generally larger size, by their lack of a limiting membrane, and by their homogeneously dense appearance in electron micrographs. Mast cell lipid bodies also differ from cytoplasmic granules in biochemistry and behavior during anti-IgE-induced degranulation (8). The data presented here reveal another difference between cytoplasmic granules and lipid bodies: lipid bodies lack a periodic, multimodal size distribution. This finding is consistent with the view that the volume of individual lipid bodies is determined by the gradual augmentation and/or mobilization of their lipid content (10).

We thank Joanne Smith for technical assistance with the electron microscopy.

These studies were supported in part by United States Public Health Service grants CA 28834, AI 20292, AI 07290, and HL 23586, and an Arthritis Foundation Postdoctoral Fellowship and a Bat-Sheba DeRothchild Fellowship to I. Hammel. This is publication No. 592 from the O'Neill Laboratories at the Good Samaritan Hospital.

REFERENCES

1. Blödner, R., P. Mühlig, and W. Nagel. 1984. The comparison by simulation of solutions of Wicksell's corpuscle problem. *J. Microsc. (Oxf.)* 135:61–74.
2. Caulfield, J. P., R. A. Lewis, A. Hein, and K. F. Austen. 1980. Secretion in dissociated human pulmonary mast cells. *J. Cell Biol.* 85:299–312.
3. Combs, J. W. 1971. An electron microscopic study of mouse mast cells arising in vivo and in vitro. *J. Cell Biol.* 48:676–684.
4. Combs, J. W., D. Lagunoff, and E. P. Benditt. 1965. Differentiation and proliferation of embryonic mast cells of the rat. *J. Cell Biol.* 25:577–592.
5. DeHoff, R. T., and F. N. Rhines. 1961. Determination of the number of particles per unit volume from measurements made on random plane sections: the general cylinder and ellipsoid. *Trans. Amer. Inst. Mineral Met. Eng.* 221:975–982.
6. Dvorak, A. M., and G. R. Dickersin. 1979. Crohn's disease, electron microscopic studies. *In* Pathology Annual, Part 2, 14. S. C. Sommers and P. P. Rosen, editors. Appleton-Century-Crofts, Connecticut. 259–306.
7. Dvorak, A. M., S. J. Galli, E. S. Schulman, L. M. Lichtenstein, and H. F. Dvorak. 1983. Basophil and mast cell degranulation: ultrastructural analysis of mechanisms of mediator release. *Fed. Proc.* 42:2510–2515.
8. Dvorak, A. M., I. Hammel, E. S. Schulman, S. P. Peters, D. W. MacGlashan, Jr., R. P. Schleimer, H. H. Newball, K. Pyne, H. F. Dvorak, L. M. Lichtenstein, and S. J. Galli. Differences in the behavior of cytoplasmic granules and lipid bodies during human lung mast cell degranulation. *J. Cell Biol.* 99:1678–1687.
9. Dvorak, A. M., M. E. Hammond, H. F. Dvorak, and M. J. Karnovsky. 1972. Loss of cell surface material from peritoneal exudate cells associated with lymphocyte-mediated inhibition of macrophage migration from capillary tubes. *Lab. Invest.* 27:561–574.
10. Fawcett, D. W. 1981. Lipid. *In* The Cell, Second Edition. W. B. Saunders Co., Philadelphia, Pennsylvania. 655–667.
11. Fullman, R. L. 1953. Measurement of particle sizes in opaque bodies. *Journal of Metals.* 5:447–452.
12. Galli, S. J., A. M. Dvorak, and H. F. Dvorak. 1984. Basophils and mast cells: morphologic insights into their biology, secretory patterns, and function. *Prog. Allergy.* 34:1–141.
13. Galli, S. J., A. M. Dvorak, J. A. Marcum, T. Ishizaka, G. Nabel, H. Der Simonian, K. Pyne, J. M. Goldin, R. D. Rosenberg, H. Cantor, and H. F. Dvorak. 1982. Mast cell clones: a model for the analysis of cellular maturation. *J. Cell Biol.* 95:435–444.
14. Hammel, I., D. Lagunoff, M. Bauza, and E. Chi. 1983. Periodic, multimodal distribution of granule volumes in mast cells. *Cell Tissue Res.* 228:51–59.
15. Henning, A., and H. Elias. 1961. Contribution to the geometry of sectioning. VI. Theoretical and experimental investigations on sections of rotatory ellipsoids. *Z. Wiss. Mikrosk.* 65:133–145.
16. Kawanami, O., V. J. Ferrans, J. D. Fulmer, and R. G. Crystal. 1979. Ultrastructure of pulmonary mast cells in patients with fibrotic lung disorders. *Lab. Invest.* 40:717–735.
17. Loud, A. V., W. C. Barany, and B. A. Pack. 1965. Quantitative evaluation of cytoplasmic structures in electron micrographs. *Lab. Invest.* 14:996–1008.
18. Matteson, D. R., M. E. Kriebel, and F. Llados. 1981. A statistical model indicates that miniature end plate potentials and unitary evoked end plate potentials are composed of subunits. *J. Theor. Biol.* 90:337–363.
19. Miller, D. C., M. M. Weinstock, and K. L. Magelby. 1978. Is the quantum of transmitters composed of subunits? *Nature (Lond.).* 274:388–390.
20. Nadelhaft, I. 1973. Measurement of the size distribution of zymogen granules from rat pancreas. *Biophys. J.* 13:1014–1029.
21. Rahaminoff, R., and Y. Yaari. 1973. Delayed release of transmitter at the frog neuromuscular junction. *J. Physiol.* 228:241–257.
22. Schulman, E. S., D. W. MacGlashan, Jr., S. P. Peters, R. P. Schleimer, H H. Newball, and L. M. Lichtenstein. 1982. Human lung mast cells: purification and characterization. *J. Immunol.* 129:2662–2667.
23. Taylor, C. C. 1982. A new method for unfolding sphere size distributions. *J. Microsc. (Oxf.)* 132:57–66.
24. Teller, D. C. Characterization of proteins by sedimentation equilibrium in the analytical ultracentrifuge. *In* Methods in Enzymology, Vol. XXVII, Part D. C. H. W. Hirs and S. N. Timasheff, editors. Academic Press Inc., New York. 346–441.
25. Weibel, E. R., and D. M. Gomez. 1962. A principle for counting tissue structures on random sections. *J. Appl. Physiol.* 17:343–348.
26. Wicksell, S. D. 1925. The corpuscle problem. *Biometrika.* 17:84–172.
27. Williams, M. A. 1977. Stereological techniques. *In* Quantitative Methods in Biology. North-Holland, New York. 5–84.